

ORIGINAL ARTICLE

Carlos E. Semino · Joshua R. Merok · Gracy G. Crane
Georgia Panagiotakos · Shuguang Zhang

Functional differentiation of hepatocyte-like spheroid structures from putative liver progenitor cells in three-dimensional peptide scaffolds

Accepted in revised form: 18 March 2003

Abstract We investigated the ability of a new type of biological material, the self-assembling peptide scaffold, to foster tissue-like function by a putative adult rat hepatocyte progenitor cell line, Lig-8. In conventional adherent petri-dish cultures, Lig-8 cells divide exponentially, express markers for definitive endoderm HNF3 β and hepatocyte lineage, including CK8 and α -fetoprotein, but lack expression of mature hepatocyte markers. However, in the three-dimensional peptide scaffold cultures, Lig-8 exhibits non-exponential cell kinetics, acquires a spheroidal morphology, and produces progeny cells with mature hepatocyte properties. The differentiated progeny cells display expression of transcription factor C/EBP α and several other indicators that suggest hepatocyte maturation, including binucleation, up-regulation of albumin, and expression of cytochrome P450s CYP1A1, CYP1A2, and CYP2E1. Moreover, all three cytochrome p450 enzyme activities are induced using 3-methylcholanthrene in these spheroids. These results suggest that a designed biological material may provide a conducive micro-environment in which putative adult progenitor cells differentiate into functional hepatocyte-like spheroid clusters. This bioengineered scaffold system provides a better physiological approach to “progenitor cell differentiation” for future biomedical and pharmaceutical applications.

Key words progenitor cell differentiation · hepatocyte-like cells · biological materials · self-assembling peptide scaffold

Introduction

Considerable progress has been made towards controlling differentiation of embryonic stem cells *in vitro*, using cellular factors that promote maturation of specific cell lineage including muscular cells, hematopoietic cells, neurons, pancreatic β -cells, etc. (Rohwedel et al., 1994; Bain et al., 1995; Palacios et al., 1995; Soria et al., 2000; Lumelsky et al., 2001). Similar advances with adult stem cells have been made but at lower rate due to their complex cell kinetics and differentiation programs (Sherley et al., 1995; Potten and Morris, 1988; Loeffler and Potten, 1997), as well as difficulties with expanding them in culture (Hoffman, 1999; Svendsen et al., 1999; Weissman, 2000; Merok and Sherley, 2001; McNiece and Briddell, 2001; Rambhatla et al., 2001). It is believed that adult stem cells divide asymmetrically to produce a new stem cell and a progenitor cell that subsequently undergoes differentiation and maturation to form functional tissues (Potten and Morris, 1988; Loeffler and Potten, 1997). In the case of adult “progenitor cell differentiation” the microenvironment or niche of the progenitor cell is likely to be one of the factors dictating the type of mature functional cells (Watt and Hogan, 2000; Spradling et al., 2001). As such, artificial microenvironments designed to produce differentiated cells from adult stem cells and progenitor cells need to support both adult progenitor cell proliferation and differentiation (Semino, 2003).

One of the goals in tissue engineering is the molecular engineering of biological materials capable of supporting growth and functional differentiation of cells and tissues in a well controlled manner. Much progress has

C. E. Semino^{1,2} (✉) · J. R. Merok^{2,3} · G. G. Crane^{2,3} ·
G. Panagiotakos¹ · S. Zhang^{1,2}

¹Center for Biomedical Engineering, ²Biotechnology Process Engineering Center, ³Biological Engineering Division, Massachusetts Institute of Technology, Cambridge, MA 02139, USA

e-mail: semino@mit.edu

Tel: +1 617 258 0249, Fax: +1 617 258 0204

been made in the last decade in developing biopolymer materials, such as polylactic acid (PLA), polyglycolic acid (PGA), hyaluronic acid, alginates, and other biocompatible scaffolds (Freed et al., 1993). In general, these polymers are composed by micro-fibers in the range of (~ 10 – $100 \mu\text{m}$) and with pores about 50 – $200 \mu\text{m}$. In this scale, cells can directly attach to the microfibers and the biological factors, mostly a few nanometer in size, may flow in and out the scaffolds freely.

We have previously described a biological scaffold, made by the interweaving of self-assembling peptide nanofibers of 10 – 20 nm in diameter, with a water content greater than 99% (5 – 10 mg/ml , w/v) (Zhang et al., 1993; 1995; Holmes et al., 2000). These nanofibers are 3 orders of magnitude thinner than other biopolymer microfibers and can thus encapsulate cells in a truly 3-dimensional environment. Several peptide scaffolds have been shown to support a variety of mature differentiated cell functions (Zhang et al., 1995; Holmes et al., 2000; Kisiday et al., 2002). However, these bioengineered materials have not been previously evaluated for their ability to support progenitor cell differentiation and function.

Here, we report the differentiation properties of a putative rat liver progenitor cell line cultured in a self-assembling peptide scaffold. The results suggest that peptide scaffolds provide a microenvironment that is conducive to normal progenitor cell kinetics and enhanced cell differentiation. The differentiated progeny displayed several characteristics of mature hepatocyte behavior, including up-regulation of albumin and expression of inducible CYP1A1, CYP1A2, and CYP2E1 cytochrome p450 enzymes that have the ability to produce complex metabolic products. It is plausible that the 3-D biological cell-scaffold culture established here would have a broad spectrum of applications for a variety of tissues, biomedical research and regenerative medicine.

Methods

Putative rat liver progenitor cell line Lig-8 and culture

The Lig-8 cell line was a generous gift from James Sherley of MIT. The derivation of putative adult rat liver progenitor Lig-8 cell line has been described in detail elsewhere (Lee et al., submitted, J. Sherley, personal communications). Lig-8 cells were maintained in regular culture dishes in DMEM supplemented with 10% dialyzed fetal bovine serum (JRH Biosciences, Lenexa, KS) and $400 \mu\text{M}$ xanthosine (Sigma).

Peptide scaffold culture

For peptide scaffold encapsulation, cells were harvested from 2-D petri-dish cultures by treatment with trypsin when they reached about 80% confluence. The released cells were washed with complete culture medium and then resuspended in 10% sucrose. Cells were counted and then resuspended in liquid RAD16-I peptide

solution (0.5% w/v, sequence: Ac-RADARADARADARADA-CONH₂ [theoretical Mass = 1712.9 ; Mass found by Mass spectra = 1713.0], SynPep Corporation, www.synpep.com, California) at a final concentration of $1,000,000 \text{ cells/ml}$. This cell concentration in three-dimensions is equivalent to a plating density of $10,000 \text{ cells/cm}^2$ with respect to maintaining constant cell-cell distances. The cell suspension was then loaded into 96-well plates ($50 \mu\text{l/well}$) and immediately equilibrated with $200 \mu\text{l}$ of culture media to initiate peptide gel formation (Kisiday et al., 2002; Caplan et al., 2002). The culture medium was changed three times during the first 60 minutes. Thereafter, peptide scaffold cultures were maintained at 37°C in a humidified incubator equilibrated with $5\% \text{ CO}_2$.

Spheroid isolation from peptide scaffold cultures

Peptide scaffold cell cultures were disrupted mechanically with a Pasteur pipette by several up and down aspirations until about 50% of the cells/clusters were extracted as determined by phase contrast microscopy. The suspension was placed in regular cell culture plates and incubated overnight in the same media at 37°C equilibrated with $5\% \text{ CO}_2$. The next day, peptide scaffold remnants were removed from attached cells by washing the culture plates with fresh media. Attached cell clusters were used for BrdU uptake, *in situ* immunofluorescence, and cytochrome p450 analyses as described below.

5'bromodeoxyuridine (BrdU) uptake analysis

BrdU was added to the culture medium at a concentration of $10 \mu\text{M}$, incubation was continued for a period of 24 h. Cells were fixed with 2% paraformaldehyde in PBS (pH 7.4) at room temperature for 2 h. Cells were treated with 2 N HCl in PBS for 30 min at 37°C . After the acid treatment, cells were equilibrated with PBS and incubated with blocking buffer (20% Calf serum; 0.1% Triton X-100; 1% DMSO in PBS) for 2 h. An anti-BrdU mouse monoclonal antibody IgG₁ FITC-conjugated (BD Pharmingen, catalog number: 33284X) was used to visualize BrdU⁺ cells with a Nikon microscope TE300 with phase contrast and epifluorescence capability. Images were stored with a Hamamatsu video camera using an Openlab data acquisition system and represent a single optical plane observed by phase contrast or fluorescence emission.

Immunofluorescence analyses

Examined cells were first fixed in 1% paraformaldehyde in PBS (pH 7.4) for 2 h at room temperature and subsequently washed several times in PBS. They were then treated with 0.1% Triton X-100 in PBS for 2 h at room temperature. Following the detergent treatment, the cells were incubated for 2 h in blocking buffer (20% Calf serum; 0.1% Triton X-100; 1% DMSO in PBS) with slow shaking. Primary antibodies were then pre-incubated in blocking buffer for 1 h at room temperature (final concentration $\sim 1 \mu\text{g/ml}$) and then added to the samples and incubated overnight at 4°C with slow shaking. The primary antibodies used were: α -fetoprotein (Santa Cruz Biotechnology, catalog number: sc-8108); rabbit polyclonal anti-rat cytochrome P450 enzyme CYP1A1 and CYP1A2 (Chemicon International Inc., AB1255); rabbit IgG anti-rat albumin-HRP (Accurate Chemicals, YNGRAALBP); rabbit IgG anti-rat C/EBP α (Santa Cruz Biotechnology, catalog number: sc-61); and mouse IgG1 monoclonal anti-rat cytokeratin 8 (Chemicon International Inc., MAB1673). Following the incubation, the samples were washed several times with blocking buffer and subsequently incubated with the appropriate secondary antibodies ($1:500$ – $1:1000$ dilution in blocking buffer) overnight at 4°C with slow shaking. The secondary antibodies used were goat anti-mouse IgG Rhodamine-conjugated (Santa Cruz Biotechnology, catalog number: sc-2029) and donkey anti-rabbit Rhodamine-conjugated (Santa Cruz Biotechnology, catalog number: sc-2095). The samples

were then washed three times with blocking buffer for 2 h. A final wash with PBS for another hour was performed before imaging as described above for BrdU analyses.

CYP1A1 and CYP1A2 activities

CYP1A1- and CYP1A2-dependent *o*-dealkylation activities on a resorufin alkyl ether substrates (7-ethoxyresorufin and 7-methoxyresorufin, respectively) were analyzed using an *in situ* fluorimetric assay (Donato et al., 1993). The reaction analyzed was the 7-ethoxyresorufin *o*-deethylation (EROD) and 7-methoxyresorufin *o*-demethylation (MROD) activities that release resorufin as product. Triplicate incubations were performed for 15 min at 37°C in presence of 3 µM of 7-ethoxyresorufin or 3 µM of 7-methoxyresorufin and 10 µM of dicumarol (Sigma), which prevents loss of resorufin due to further metabolism by cytosolic oxidoreductases. The resorufin product was measured by the increase fluorescence intensity with excitation/emission filters of 530 nm/590 nm. Resorufin product concentration was calculated based on a resorufin standard curve developed in the respective cell culture medium. Assayed cell number was determined by hemocytometer counting of trypsinized cells after the assay was completed. Enzymatic activity was expressed in units of fmol resorufin produced/cell/h.

3-methylcholantrene (3-MC) treatment

The aromatic hydrocarbon 3-MC (Sigma) was added to the culture media of cells in adherent culture or isolated peptide scaffold spheroids at a final concentration of 2 µM starting on the fourth day of culture. Thereafter, every other day 50% of the culture medium was exchanged with fresh medium containing 3-MC.

Caffeine-8-[¹⁴C] metabolism

Lig 8 cells in adherent culture and isolated peptide scaffold spheroids (cultured in peptide scaffold for 4 days old) were incubated in absence or presence of 3-methylcholantrene (3-MC) for 48 h. Cells were incubated for additional 24 h in medium containing 0.4 mM caffeine-8-[¹⁴C] (53 mCi/mmol; 20 µCi/ml, Sigma). After the incubation, half of the cells from each sample were counted, and the other half was heated to 100°C for 4 min. The treated material was then sonicated for 5 min to facilitate solubilization of the reaction products. The sonicated cell extracts were centrifuged at 14,000 rpm, and 5 µl aliquot of the supernatant (5%) was spotted on a silica-gel thin-layer chromatography plate (EM Science, New Jersey; Silica Gel 60 F₂₅₄) with the following standards (Sigma): caffeine (1,3,7-trimethylxanthine), theophylline (1,3-dimethylxanthine), theobromide (3,7-dimethylxanthine), paraxanthine (1,7-dimethylxanthine), 3-methylxanthine, and xanthine. The plate was developed with chloroform:acetone (1:1). Standards were visualized with short wave ultraviolet light (UV, 254 nm, Spectrolite ENF-260C), and radioactive metabolites detected by autoradiography with X-ray film (BioMax, Kodak). Radioactivity in metabolites that co-chromatographed with theobromide, theophylline, and paraxanthine were recovered by scraping and counted in a scintillation counter. Based on the recovery of radioactivity, production rates for the respective compounds were expressed as pmol/day/10⁶ cells.

Cell viability and apoptosis

Cell viability was assessed on spheroid colonies with Dead/Live staining (Molecular Probes, Eugene, OR; catalog number: L-3225). Cell membrane-permeant calcein AM is cleaved by esterases in live cells to yield cytoplasmic green fluorescent, and the membrane impermeant ethidium homodimer-1 labels nucleic acids of membrane compromised cells with red fluorescence. Apoptosis was visualized

by nuclear staining with DAPI dye. Apoptotic cells are easy to detect by morphological analysis of the nuclei, where they normally present granular staining when apoptotic.

Results

Cell kinetics of a putative adult rat progenitor cell line cultured in 3-D RAD16-I peptide scaffold

We compared the cell kinetics of the adult hepatocyte progenitor cell line Lig-8 grown in standard 2-D culture dishes to their kinetics after encapsulation into 3-D RAD16-I peptide scaffolds. Cells were cultured in peptide scaffolds using their routine culture medium over a period of 4 days before isolation for quantitative analyses. Cell clusters obtained in 3-D peptide scaffolds were isolated by mechanical disruption of the matrix (easily done due to the non-covalent nanofiber network and extremely high water content, 99.5%) and counted with a hemacytometer. Cell numbers were counted as the number of cells per adherent colony grown in culture dishes, or per isolated scaffold cell cluster (i.e. scaffold “spheroids”; Table 1). Most spheroids were isolated intact by this procedure.

After the first 24 h, the number of cells in colonies grown in culture dishes increased exponentially with a calculated doubling time (DT) of 24 h (Table 1). However, in the 3-D peptide scaffold, the division kinetics of Lig-8 cells was different. During the first 24 h in scaffold culture, the cells initiated the formation of very small clusters of 2 to 6 cells (4.1 ± 1.9 cells/cluster; Fig. 1A, B; Table 1). In the following days, many of the bigger clusters adopted a spheroidal morphology (Fig. 1C, D). Interestingly, the average number of cells in the spheroids increased linearly when compared to adherent 2-D cultures, with a DT close to 38 h (Table 1).

The change in the cell division kinetics of the spheroids could be explained by an increase in the cell generation time (GT), by cell division arrest of some cells in the clusters, or both. Trypan blue dye exclusion analyses showed that the viability of cells in scaffold cultures was close to ~90%.

The thymidine analog 5-bromodeoxyuridine (BrdU) was used to evaluate the proportion of proliferative cells in the peptide scaffold cultures. Cells were labeled for 24 h with BrdU (i.e. about 1 doubling time for Lig-8 cells in adherent culture) to label the population of cycling cells. Due to the 3-dimensional topology of scaffold spheroids, it was difficult to quantify accurately the number of BrdU-positive (BrdU⁺) cells *in situ* (not shown). Therefore, analyses were performed with isolated spheroids attached on regular culture dishes that had formed “spheroid-colonies” (see Methods). As expected, the BrdU⁺ fraction of colonies in adherent 2-D culture was very high (>95%; see Fig. 1E, F). In con-

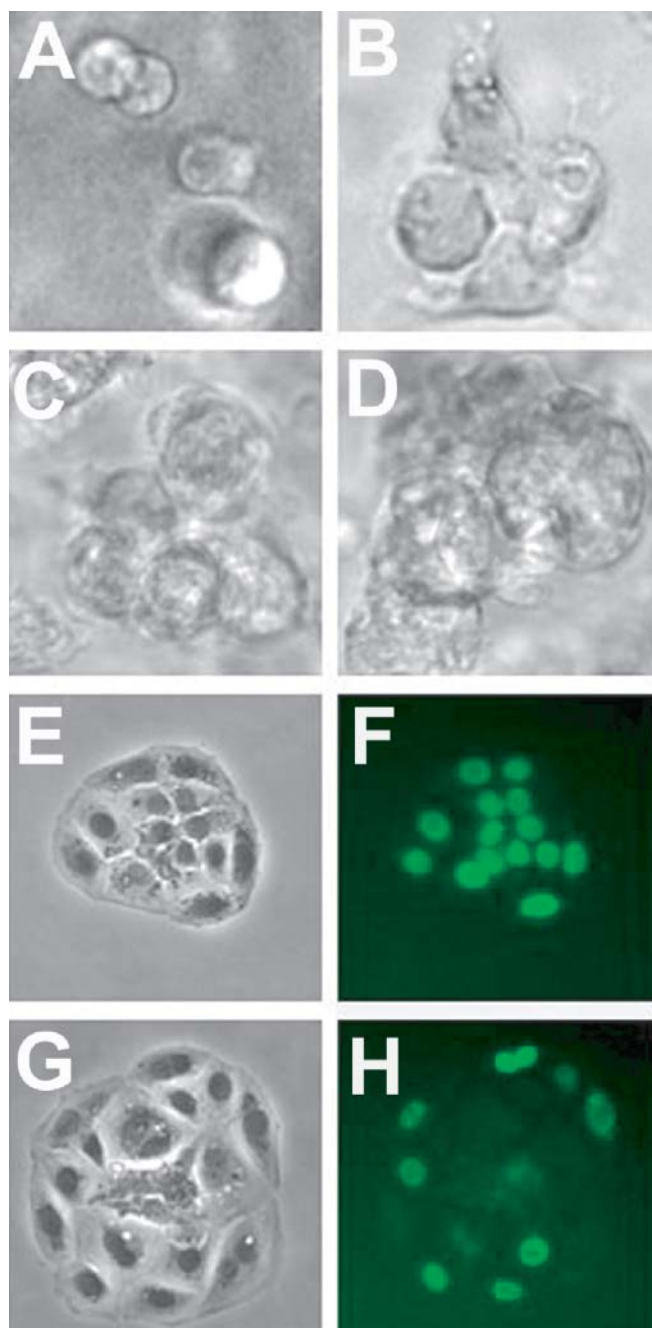


Fig. 1 Cell kinetics of Lig-8 adult hepatocyte stem cells cultured in RAD16-I peptide scaffolds. Lig-8 cells were grown in adherent culture or in RAD16-I peptide scaffolds for a period of 96 h (see Methods). **A**, Cells directly after encapsulation in the peptide scaffold; **B**, after 24 h, cells form small clusters of about 4 cells; **C**, spheroid morphology develops after 48 h of peptide scaffold culture (clusters of 5–6 cells); **D**, spheroid morphology after 96 h in peptide scaffold culture (clusters of 10–14 cells). To evaluate the cycling cell fraction, adherent cultures were incubated for 24 h in the presence of 10 μ M of 5'-bromodeoxyuridine (BrdU), and cycling cells were detected by direct anti-BrdU immunofluorescence (see Methods). Spheroids in peptide scaffold were transferred to adherent culture (see Methods) for BrdU uptake analysis. **E**, 48 h adherent cell colony (phase contrast); **F**, anti-BrdU immunofluorescence for the colony in **E**; **G**, a spheroid after 96 h of peptide scaffold culture (phase contrast); **H**, anti-BrdU immunofluorescence for the colony in **G**. **A–D** 400 \times magnification; **E–H**, 200 \times magnification.

Table 1 Lig-8 cell kinetics in standard adherent culture versus in RAD16-I peptide scaffold culture^w

Culture time (h)	Number of cells per colony or spheroid (mean \pm sd) [§]	
	Adherent Culture (n = 3)	Hydrogel Spheroids (n = 8)
24	5.3 \pm 1.8	4.1 \pm 1.9
48	11 \pm 2.0	6.3 \pm 1.1
96	41 \pm 5.4 (24h) ^δ	15 \pm 3.8 (38h)

^w Lig-8 cells were cultured in regular 6-well culture dishes (n = 3) and plated at an initial density of \sim 1,000 cells/cm² or encapsulated into RAD16-I peptide scaffold (0.5% w/v) at initial concentration of \sim 100,000 cell/ml (n = 8; see Methods), contained into culture inserts (see Methods). Cells were grown in DMEM supplemented with 10% dialyzed fetal bovine serum and xanthosine (400 μ M), conditions that promote exponential cell kinetics by Lig-8 cells (Lee et al., submitted). Cells were cultured for the indicated times, and the number of cells per colony or spheroid (isolated from peptide scaffold) was counted by stereo microscopy. Ten colonies or spheroids were randomly selected for analysis from each of *n* independent cultures (i.e., a total of 30 colonies at each time point for adherent cultures and 80 spheroids from peptide scaffold cultures).

[§] Data is expressed as mean cell number per colony \pm standard deviation (sd).

^δ The average colony doubling time (DT) is shown in parentheses.

trast, a fraction of the cells in the scaffold spheroids (<50%) incorporated BrdU. This is consistent with the hypothesis that many cells in the peptide scaffolds became mitotically arrested (Fig. 1G, H). In addition, cell viability (Dead/Live test, Molecular Probes) and apoptosis analysis (nuclear DAPI staining) performed in the spheroid-colonies confirmed few nonviable cells (<3%) and no evidence of apoptotic nuclei (not shown), suggesting that the linear cell growth rate in the peptide scaffold cultures was not due to a programmed cell death process.

Interestingly, the phenotype of the non-cycling BrdU⁻ (BrdU-negative) cells in the spheroid-colonies was remarkably different than in the cycling cells. They exhibited increased cell size with a high incidence of binucleation (Fig. 1G, H), a characteristic of differentiated hepatocytes. This latter finding was the first indication that the peptide scaffold promotes hepatocyte differentiation of Lig-8 cells.

Promotion of hepatocyte differentiation in three-dimensional (3-D) RAD16-I peptide scaffolds

In standard petri-dish cultures, Lig-8 cells express the markers for definitive endoderm HNF3 β and hepatocyte lineage, including α -fetoprotein (Shiojiri et al., 1991) and albumin, but did not express markers specific for other non-hepatocyte liver cell populations, such Kupffer cells or stellate cells (Table 2). We analyzed differences in the expression of several cellular markers of hepatocyte dif-

Table 2 Induction of hepatocyte phenotypes in RAD16-I peptide scaffolds

Marker [¶]	Standard Culture Dish	Peptide Scaffold Spheroids [§]
<i>Hepatocyte progenitor</i>		
α-Fetoprotein	+	+
CK8 (also mature hepatocytes)	+	+
<i>Definitive endoderm</i>		
HNF3β*	+	NA
<i>Non-hepatocyte liver cell population</i>		
ED1 (Kupffer cells)*	-	NA
GFAP (stellate cells)*	-	NA
<i>Endodermal (liver) development</i>		
C/EBPα	-	+++
<i>Mature hepatocyte</i>		
Albumin	-/+	+++
CYP1A1/CYP1A2	-/+	++
CYP2E1	-	++
Binucleated cells	-	++
<i>Functional hepatocyte</i>		
3-MC inducible CYP1A1	-	+
3-MC inducible CYP1A2	-	++
Caffeine metabolism (CYP1A2/2E1)	-	++

[¶] Quantification terms for marker expression: (-), not detected; (-/+), very low; (+), low; (++), medium; (+++), high expression.

[§] Cells were either grown in standard adherent culture or grown in peptide scaffold and then transferred to adherent culture for analysis as described in Methods.

* Lee et al., submitted

NA, not analyzed.

differentiation after culturing Lig-8 cells in either 2-D petri dishes or in 3-D RAD16-I peptide scaffolds. These include the liver developmental marker C/EBPα, a CCAAT enhanced-binding protein highly expressed in hepatocytes and other endodermal tissues (Wang et al., 1995); the hepatocyte markers albumin (Houssaint, 1980) and cytokeratin 8 (CK8) (Van Eyken et al., 1988; Bouwens et al., 1994; Grisham and Thorgeirsson, 1997); the expression and activity of cytochromes P450 such as CYP1A1 and CYP1A2; and presence of binucleated cells (Table 2).

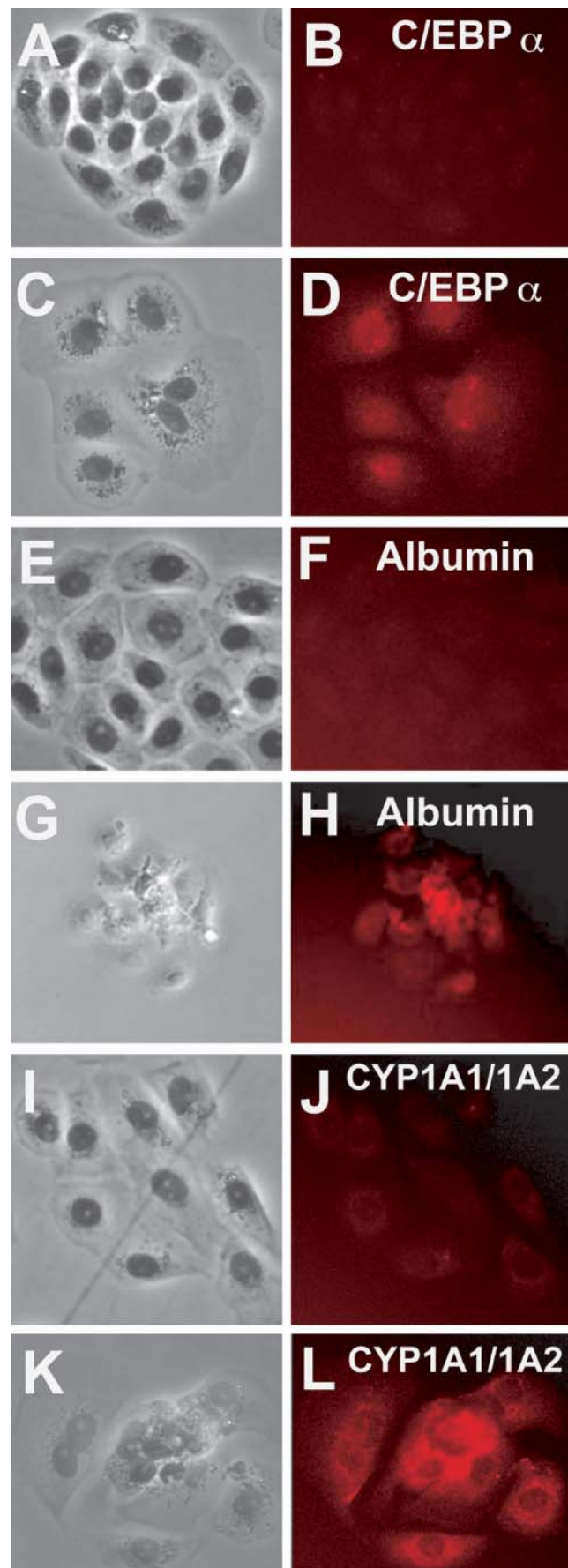


Fig. 2 Promotion of hepatocyte differentiation by RAD16-I peptide scaffold. Lig-8 progenitor cells were cultured in adherent culture or in RAD16-I peptide scaffold. Spheroids were isolated and analyzed approximately 16 h after transfer to adherent culture. **A E, I**, adherent cell colonies (phase contrast); **B F, J**, respective *in situ* immunofluorescence for adherent colonies with anti-C/EBPα, anti-albumin, and anti-CYP1A1/1A2 antibodies; **C G, K**, isolated peptide scaffold spheroids (phase contrast; note binucleated cells); **D H, L**, respective *in situ* immunofluorescence for isolated peptide scaffold spheroids with anti-C/EBPα, anti-albumin, and anti-CYP1A1/1A2 antibodies.

The developmental marker C/EBP α was highly expressed in all nuclei of spheroid cells isolated from 3-D peptide scaffold cultures, whereas no detectable expression in Lig-8 2-D petri culture dish colonies was found (compare Fig. 2B and D). Other hepatocyte markers, such as albumin and the cytochrome CYP1A1 and CYP1A2, were also highly expressed in 3-D scaffold spheroids (Fig. 2E-L and Table 2). Another typical characteristic of hepatocyte differentiation and maturation was the production of large binucleated cells found in most spheroid colonies isolated from the 3-D scaffold cultures (Figs. 1 and 2; Table 2). In addition, the expression of α -fetoprotein and CK8 did not change after culturing Lig-8 cells in peptide scaffolds (Table 2). α -fetoprotein is expressed in hepatoblasts, and CK8 is expressed in both hepatoblasts and mature hepatocytes (Grisham and Thorgeirsson, 1997), suggesting the presence of some incomplete differentiated cells in the spheroid-colonies.

Finally, to study the fraction of cells in the spheroid colonies, regardless if dividing or not, undergoing differentiation, we performed a double staining experiment for BrdU and CYP1A1/1A2 or BrdU and C/EBP α , respectively. Results suggest that all cells express the differentiation markers independently of their mitotic activity (Fig. 3). This implies that a proportion of cells in the spheroid colony stop dividing while the entire population becomes committed to differentiation.

Complex metabolic responses and functions of cellular spheroids in RAD16-I peptide scaffold

Our findings were consistent with the possible differentiation of hepatocyte-like cells (Potten, 1988; Loeffler and Potten, 1997) by Lig-8 cells upon culture in 3-D peptide scaffolds. Although these spheroids in the peptide scaffold lacked the full range of liver tissue components (e.g. endothelium), they presented a basic architectural unit of differentiating cells. Given these features, we evaluated whether the 3-D peptide scaffold spheroids might have functional capabilities of mature hepatocytes.

The up-regulated expression of CYP1A1 and CYP1A2 proteins in scaffold spheroids predicted the presence of the corresponding enzymatic activities (Fig. 2I-L, Table 2). Using fluorimetric assays (Donato et al., 1993), we tested for CYP1A1 and CYP1A2 enzymatic activities in adherent cell cultures and isolated scaffold spheroids over a ten-day period (see Methods). Lig 8 cells in culture dishes had weak CYP1A1 and CYP1A2 activity (Fig. 4A and B). When cells were treated with the polycyclic aromatic hydrocarbon 3-methylcholanthrene, only the CYP1A1 activity exhibited modest elevation (3-MC; Fig. 4A). 3-MC is a known inducer of CYP1A1 and CYP1A2 expression in liver hepatocytes

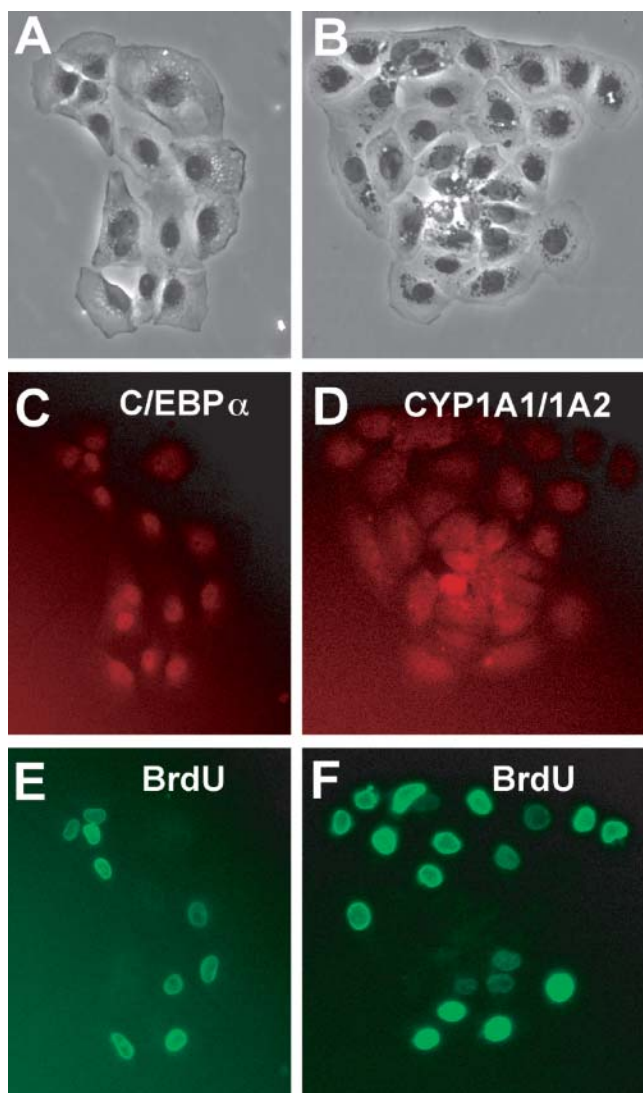


Fig. 3 All cells in Spheroid colonies, arrested or not, undergo differentiation. Lig-8 cells were cultured in RAD16-I peptide scaffold. Spheroids were isolated, transferred to adherent cultures, and incubated with BrdU for 24 h. **A**, spheroid colony (phase contrast); **C**, same optical layer as **A** immunostained for C/EBP α (red); **E**, same optical layer as **A** immunostained for BrdU (green). **B**, spheroid colony (phase contrast); **D**, same optical layer as **B** immunostained for CYP1A1/1A2 (red); **F**, same optical layer as **B** immunostained for BrdU.

via the ligand-activated nuclear receptor AHR (Jones et al., 1985; Burbach et al., 1992).

In contrast to results with Lig-8 cells in 2-D petri dish culture, after only four days of 3-D peptide scaffold culture, basal CYP1A1 activity in isolated cellular spheroids increased significantly, reaching a >8-fold higher level by 10 days (Fig. 4C, circles). CYP1A2 activity showed a similar degree of elevation but with faster kinetics (Fig. 4D, circles). Moreover, both classes of p450 enzymes exhibited marked elevations in activity when cells were cultured in peptide scaffold containing 3-MC (Fig. 4C and D; squares). CYP1A1 and CYP1A2 activ-

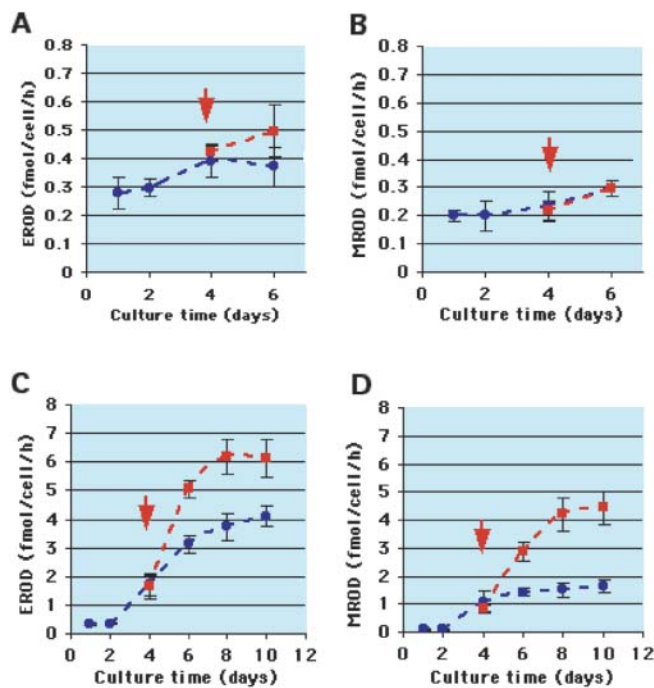


Fig. 4 Induction of CYP1A1 and CYP1A2 activities by 3-methylcholantrene (3-MC) in peptide scaffold spheroids. Lig-8 hepatocyte progenitor cells in adherent culture (A and B) or isolated peptide scaffold spheroids (C and D) were assayed for CYP1A1 and CYP1A2 activities after culture in the presence (■) or absence (●) of the polycyclic aromatic hydrocarbon 3-MC. For C and D, each time point indicates the total time for peptide scaffold culture and spheroid isolation. CYP1A1 and CYP1A2 activities were detected by measuring the production of fluorescent resorufin after incubating cells with 7-ethoxyresorufin (EROD; A and C) or 7-methoxyresorufin (MROD; B and D), respectively (see Methods). Data are plotted as the mean value of triplicate assays with the sample standard deviation. Arrows indicate the time when 3-MC was added to adherent cells or spheroids in peptide scaffold prior to their isolation for assay. 3-MC was maintained throughout the isolation and assay periods.

ities increased maximally, 150% and 300%, respectively, when compared to the untreated cellular spheroids in peptide scaffold. Both the basal and 3-MC induced p450 activities were maintained for at least 72 hours, the longest period evaluated.

As a test of the ability of cellular spheroids in peptide scaffold to perform complex metabolic conversions, we examined their ability to convert caffeine (1,3,7-trimethylxanthine) into its common metabolites. CYP1A2 is known to specifically catalyze the N_3 -demethylation of caffeine to produce paraxanthine (1,7-dimethylxanthine) (Butler et al., 1989). Radio-labeled caffeine (caffeine-8- ^{14}C) was added to Lig-8 cells in adherent culture or to isolated cellular spheroids in 3-D peptide scaffold as described in Methods. After a 24-hour incubation period, ^{14}C -labeled cellular metabolites were analyzed by separating total cell extracts by thin layer chromatography (see Methods).

Under normal culture conditions, ^{14}C -labeled meta-

bolites were only detected in extracts of peptide scaffold spheroids (Table 3). As expected because of the previous demonstration of CYP1A2 activity, caffeine N_3 -demethylating activity was noted by the appearance of paraxanthine-8- ^{14}C . In addition, two other N -demethylating activities were detected, N_1 -demethylation and N_7 -demethylation, producing theobromide (3,7-dimethylxanthine) and theophylline (1,3-dimethylxanthine), respectively (Table 3). The production of these two metabolites indicates the action of the N -demethylating activity, CYP2E1, previously described to be up-regulated by 3-MC (Ratanasavanh et al., 1990; Roberts et al., 1994). The production rate of all three identified metabolites increased 3–6-fold (Table 3) when peptide scaffold spheroids were developed in the presence of 3-MC. In addition, with caffeine as the substrate, even cells in 2-D adherent culture showed a marked increase in CYP1A2 activity after 3-MC exposure (> 30-fold elevation; Contrast Table 3 to Fig. 4B, squares). Altogether, these results demonstrate the potential for hepatocyte progenitor cellular spheroids developed in 3-D peptide scaffolds to provide complex metabolic responses and functions characteristic of differentiated hepatocytes.

Discussion

Our results suggest that culturing Lig-8 cells in a 3-dimensional self-assembling peptide scaffold micro-environment appears to be a sufficient condition to promote hepatocyte differentiation.

The 3-D peptide scaffold used in the present study differs significantly from other biopolymer-based biomaterials in several distinctive ways. Most currently used biopolymers have fiber sizes generally within a 10–100 micron range of diameter, which is similar to the average diameter of many types of mammalian cells. For these fiber sizes, several investigators have covalently linked cell adhesion motif RGD to the biopolymer to enhance cell-material interactions (Cook et al., 1997). However, because of the size of the fibers, cells essentially interface with a 2-dimensional curved surface. In contrast, the peptide scaffold spontaneously self-assembles into nanofibers (i.e. 10–20 nm in diameter) (Zhang et al., 1993) that are highly hydrated, trapping water at total volume contents of 99.5%. In such a “nanofiber scaffold”, cells are embodied in a truly 3-dimensional environment.

We observed that the peptide scaffold allowed Lig-8 cells to organize into clusters or cellular spheroids. Because the peptide scaffold pore size is within a 50–200 nm range, thus creating a nanofiber environment, it permits slow diffusion of small molecules, metabolites and macromolecules such as gases, nutrients, and growth factors. However, the route of the delivery of such constituents to cells may differ significantly from that in 2-D adherent or suspension culture systems. For example, transport of important cellular effector molecules to and

Table 3 Caffeine metabolism^δ by RAD16-I peptide scaffold spheroids

Metabolite	CYP	Activity	Adherent Culture		Peptide Scaffold	
			- 3-MC	+ 3-MC	- 3-MC	+ 3-MC
Paraxanthine [§]	1A2	<0.01 ^ψ	0.34, 0.30	1.3, 1.7	5.4, 5.8	
Theophylline	2E1	<0.01	0.03, 0.02	0.54, 0.68	3.6, 3.9	
Theobromide	2E1	<0.01	<0.01		0.80, 1.1	5.6, 6.3

^δ Caffeine (caffeine-8-[¹⁴C]) was incubated in with Lig-8 cells in adherent culture or with isolated peptide scaffold spheroids with (+) or without (-) prior exposure to 3-methylcholantrene (3-MC) as described in Methods.

[§] Metabolite data are presented as the rates of production in units of pmol/day/10⁶ cells. Results from duplicate analyses are given.

^ψ 0.01 pmol/10⁶ cells/day was the limit of detection in the analyses.

from cells might be facilitated by the creation of local microenvironments composed of secreted paracrine and autocrine factors and extracellular matrix (ECM) components that may absorb to peptide scaffold nanofibers. Moreover, nanofiber three-dimensional contouring of the cell membrane might also have consequences that affect the way in which cellular receptors for growth factors/cytokines and ECM proteins and proteoglycans interact with signaling ligands (Semino, 2003).

The putative rat liver progenitor cells were also cultured in other peptide scaffolds, such as KLD12 (AcN-KLDLKLKLDL-CONH₂) and KFE8 (AcN-KF-EFKFEF-CONH₂). These peptides produce stiffer scaffolds than RAD16-I (used in this work), due to the high content of hydrophobic residues. As a consequence, Lig-8 cells did not grow well, exhibiting in small spheroids with low hepatic differentiation phenotype (not shown). This indicates that the design in the peptide selected is important for obtaining the right culture conditions. In addition, 0.5% soft agarose gel (a microfiber scaffold commonly used in tissue culture) was used as a control to culture Lig-8 cells in a three-dimensional system. The microfiber network of soft agarose is stiffer than the peptide nanofiber scaffold, therefore cells cannot migrate nor form bigger cellular clusters. Moreover, no EROD activity (7-ethoxyresorufin *o*-deethylation) was detected from Lig-8 cells cultured in soft agarose gels suggesting no differentiation in such culture conditions (not shown). Finally, experiments with gelatin (1–5%) were also performed to compare experiments in peptide scaffold hydrogel with other nanofiber scaffolds. In all cases, cell cultures ended in the bottom of the dishes forming a monolayer with very low EROD activity (not shown). This result suggests that the establishment of a three-dimensional environment is a key element for proper Lig-8 differentiation in the conditions tested.

We observed that peptide scaffold spheroids exhibit detectable and inducible xenobiotic metabolizing/detoxifying enzyme activities including CYP1A1 and CYP1A2 enzymes. In addition, another metabolizing activity was evident in the three-dimensional cultures after exposure to 3-methylcholanthrene (3-MC), CYP2E1. This enzyme is involved in *N*₁- and *N*₇-demethylation of caffeine to produce theobromide (3,7-dimethylxanthine) and theo-

phylline (1,3-dimethylxanthine), respectively (Table 3). The activation of CYP1A1, CYP1A2, CYP2E1 by 3-MC in the Lig-8 peptide scaffold cultures was previously observed in primary cultures of human hepatocytes (Butler et al. 1989; Ratanasavanh et al., 1990; Roberts et al., 1994).

Moreover, if using human adult hepatic progenitor cells, it may not only be possible to develop human hepatic spheroids in peptide scaffolds with greater predictive value for human toxicity and drug efficacy, but also, at the same time, alleviate the acute needs to use animals for drug and cosmetic tests. The molecular-designed peptide scaffolds may also be useful in regenerative and reparative medicine.

Acknowledgements We are grateful to John Kisiday and Alan Grodzinsky for providing initial instructions in peptide scaffold encapsulation techniques and James Sherley for generously providing putative rat liver progenitor Lig-8 cells and helpful discussions. We would also like to thank Douglas Lauffenburger for critical review of the manuscript. This work was supported primarily by the Engineering Research Centers Program of the National Science Foundation under NSF Award Number 9843342. Correspondence regarding Lig-8 cells should be addressed to James Sherley (jsherley@mit.edu).

References

- Bain, G., Kitchens, D., Yao, M., Huettner, J.E. and Gottlieb, D.I. ((1994).) Embryonic stem cells express neuronal properties in vitro. *Dev Biol* 168:342–357.
- Bouwens, L., Wang, R.N., De Blay, E., Pipeleers, D.G. and Kloppel, G. (1994) Cytokeratins as markers of ductal cell differentiation and islet neogenesis in the neonatal rat pancreas. *Diabetes* 43:1279–1283.
- Burbach, K.M., Poland, A. and Bradfield, C.A. (1992) Cloning of the Ah-receptor cDNA reveals a distinctive ligand-activated transcription factor. *Proc Natl Acad Sci USA* 89:8185–8189.
- Butler, M.A., Iwasaki, M., Guengerich, F.P. and Kadlubar, F.F. (1989) Human cytochrome P-450PA (P-450IA2), the phenacetin *O*-deethylase, is primarily responsible for the hepatic 3-demethylation of caffeine and *N*-oxidation of carcinogenic arylamines. *Proc Natl Acad Sci USA* 86:7696–7700.
- Cook, A.D., Hrkach, J.S., Gao, N.N., Johnson, I.M., Pajvani, U.B., Cannizzaro, S.M. and Langer, R. (1997) Characterization and development of RGD-peptide-modified poly(lactic acid-co-lysine) as an interactive, resorbable biomaterial. *C J Biomed Mater Res* 35:513–23.

- Donato, M.T., Gomez-Lechon, M.J. and Castell, J.V. (1993) A microassay for measuring cytochrome P450IA1 and P450IIB1 activities in intact human and rat hepatocytes cultured on 96-well plates *Anal Biochem* 213:29.
- Freed, L.E., Marquis, J.C., Nohria, A., Emmanuel, J., Mikos, A.G. and Langer, R. (1993) Neocartilage formation in vitro and in vivo using cells cultured on synthetic biodegradable polymers. *J Biomed Mater Res* 27:11–23.
- Grisham, J.W. and Thorgeirsson, S.S. (1997) Liver stem cells. In: Potten, C.S. (ed.) *Stem cells*. Academic Press, London, pp 233–282.
- Hoffman, R. (1999) progress in development of systems for in vitro expansion of human hematopoietic stem cells. *Curr Opin Hemato* 16:187–191.
- Holmes, T., Delacalle, S., Su, X., Rich, A. and Zhang, S. (2000) Extensive neurite outgrowth and active neuronal synapses on peptide scaffolds. *Proc Natl Acad Sci USA* 97:6728–6733.
- Houssaint, E. (1980) Differentiation of the mouse hepatic primordium. I. An analysis of tissue interactions in hepatocyte differentiation. *Cell Differ* 9:269–279.
- Jones, P.B.C., Galeazzi, D.R., Fisher, J.M. and Whitlock, J.P. Jr. (1985) Control of cytochrome P1–450 gene expression by dioxin. *Science* 277:1499–1502.
- Kisiday, J., Jin, M., Kurz, B., Hung, H., Semino, C., Zhang, S. and Grodzinsky, A.J. (2002) Self-assembling peptide hydrogels fosters chondrocyte extracellular matrix production and cell division: Implications for cartilage tissue repair. *Proc Natl Acad Sci USA* 99:9996–10001.
- Loeffler, M. and Potten, C.S. (1997) Stem cells and cellular pedigrees – a conceptual introduction. In: Potten, C.S. (ed.) *Stem Cells*. Harcourt Brace and Co., San Diego, CA, pp 1–28.
- Lumelsky, N., Blondel, O., Laeng, P., Velasco, I., Ravin, R. and McKay, R. (2001) Differentiation of embryonic stem cells to insulin-secreting structures similar to pancreatic islets. *Science* 292:1389–1394.
- McNiece, I. and Briddell, R. (2001) Ex vivo expansion of hematopoietic progenitor cells and mature cells. *Exp Hematol* 29:3–11.
- Merok, J.R. and Sherley, J.L. (2001) Breaching the kinetic barrier to in vitro somatic stem cell propagation. *J Biomed Biotech* 1:25–27.
- Palacios, R., Golunski, E. and Samaridis, J. (1995) In vitro generation of hematopoietic stem cells from an embryonic stem cell line. *Proc Natl Acad Sci USA* 92:7530–7534.
- Potten, C.S. and Morris, R.J. (1988) Epithelial stem cells in vivo. *J. Cell Sci Suppl* 10:45–62.
- Rambhatla, L., Bohn, S.A., Stadler, P.B., Boyd, J.T., Coss, R.A. and Sherley, J.L. (2001) Cellular senescence: ex vivo p53-dependent asymmetric cell kinetics. *J Biomed Biotech* 1:28–37.
- Ratanasavanh, D., Berthou, F., Dreano, Y., Mondine, P., Guillouzo, A. and Riche, C. (1990) Methylcholanthrene but not phenobarbital enhances caffeine and theophylline metabolism in cultured adult human hepatocytes. *Biochem Pharmacol* 39:85–94.
- Roberts, E.A., Furuya, K.N., Tang, B.K. and Kalow, W. (1994) Caffeine biotransformation in human hepatocyte lines derived from normal liver tissue. *Biochem Biophys Res Commun* 201:559–566.
- Rohwedel, J., Maltsev, V., Sober, E., Arnold, H.H., Hescheler, J. and Wobus, A.M. (1994) Muscle cell differentiation of embryonic stem cells reflects myogenesis in vivo: developmentally regulated expression of ionic currents. *Dev Biol* 164:87–101.
- Semino, C.E. (2003) Can we build artificial stem cell compartments? *J Biomed Biotech* 3 (In press).
- Sherley, J.L., Stadler, P.B. and Johnson, D.R. (1995) Expression of the wild-type p53 antioncogene induces guanine nucleotide-dependent stem cell division kinetics. *Proc Natl Acad Sci USA* 92:136–140.
- Shiojiri, N., Lemire, J.M. and Fausto, N. (1991) Cell lineages and oval cell progenitors in rat liver development. *Cancer Res* 51:2611–2620.
- Soria, B., Roche, E., Berna, G., Leon-Quinto, T., Reig, J.A. and Martin, F. (2000) Insulin-secreting cells derived from embryonic stem cells normalize glucemia in streptozotocin-induced diabetic mice. *Diabetes* 49:157–162.
- Spradling, A., Drummond-Barbosa, D. and Kai, T. (2001) Stem cells find their niche. *Nature* 414:98–104.
- Svendsen, C.N., Caldwell, M.A. and Ostenfeld, T. (1999) Human neural stem cells: isolation, expansion and transplantation. *Brain Pathol* 9:499–513.
- Van Eyken, P., Sciote, R. and Desmet, V. (1988) Intrahepatic bile duct development in the rat: A cytokeratin-immunohistochemical study. *Lab Invest* 59:52–59.
- Wang, N.D., Finegold, M.J., Bradley, A., Ou, C.N., Abdelsayed, S.V., Wilde, M.D., Taylor, L.R., Wilson, D.R. and Darlington, G.J. (1995) Impaired energy homeostasis in C/EBP alpha knock-out mice. *Science* 269:1108–1112.
- Watt, F.M. and Hogan, B.L.M. (2000) Out of Eden: Stem cells and their niches. *Science* 287:1427–1430.
- Weissman, I.L. (2000) Stem cells: units of development, units of regeneration, and units of evolution. *Cell* 100:157–168.
- Zhang, S., Holmes, T., Lockshin, C. and Rich, A. (1993) Spontaneous assembly of a self-complementary oligopeptide to form stable macroscopic membrane. *Proc Natl Acad Sci USA* 90:3334–3338.
- Zhang, S., Holmes, T.C., DiPersio, C.M., Hynes, R.O., Su, X., Rich, A. (1995) Self-complementary oligopeptide matrices support mammalian cell attachment. *Biomaterials* 16:1385–1393.